Scale effects in the physical modelling of seabed scour

J Sutherland
R J S Whitehouse

Report TR 64
September 1998

HR Wallingford

Contract

Prepared by *James Sutherland*

(name)

Project Engineer

(Title)

Approved by *Richard Whitehouse*

(name)

Project Manager

(Title)

Date *1st October 1998*

Summary

Scale effects in the physical modelling of seabed scour

J Sutherland, R J S Whitehouse

Report TR 64
September 1998

This report describes and comments on scale effects in the physical modelling of seabed scour around coastal and offshore man-made structures. It has been produced within the framework of the EC funded project Scour Around Coastal Structures (SCARCOST). The intention is to highlight the scaling problems that are faced in mobile bed studies of scouring, to comment on them and to refer to the latest findings from researchers who have looked at scale effects in particular problems. The report is not intended to provide an introduction to the scale modelling of waves or waves around structures with fixed beds, although the main hydrodynamic parameters are introduced as they are also important for mobile bed studies. The report concentrates on flow and scour processes, the areas covered by Task 1 of SCARCOST. The response of the bed is covered in Task 2 and is considered only briefly here.

The main non-dimensional numbers for short wave fixed-bed model scaling are introduced for reference. Then some basic scaling issues for mobile sediment models are outlined, followed by an introduction to the main non-dimensional parameters used in sediment transport. Descriptions of hydrodynamic scaling, the scaling of sediment, the possible effects of ripples, bed response and structural response follow. Then come descriptions of the problems associated with scaling the scour at different types of structure. The specific structure types are vertical piles, groups of piles, horizontal pipelines, vertical breakwaters, sloping breakwaters and rubble mound breakwaters. The report finishes with some comments on the timescales of scour, scaling lengths, the effect of the initial bed profile and the difficulties of separating the scour due to structures from the beach response.
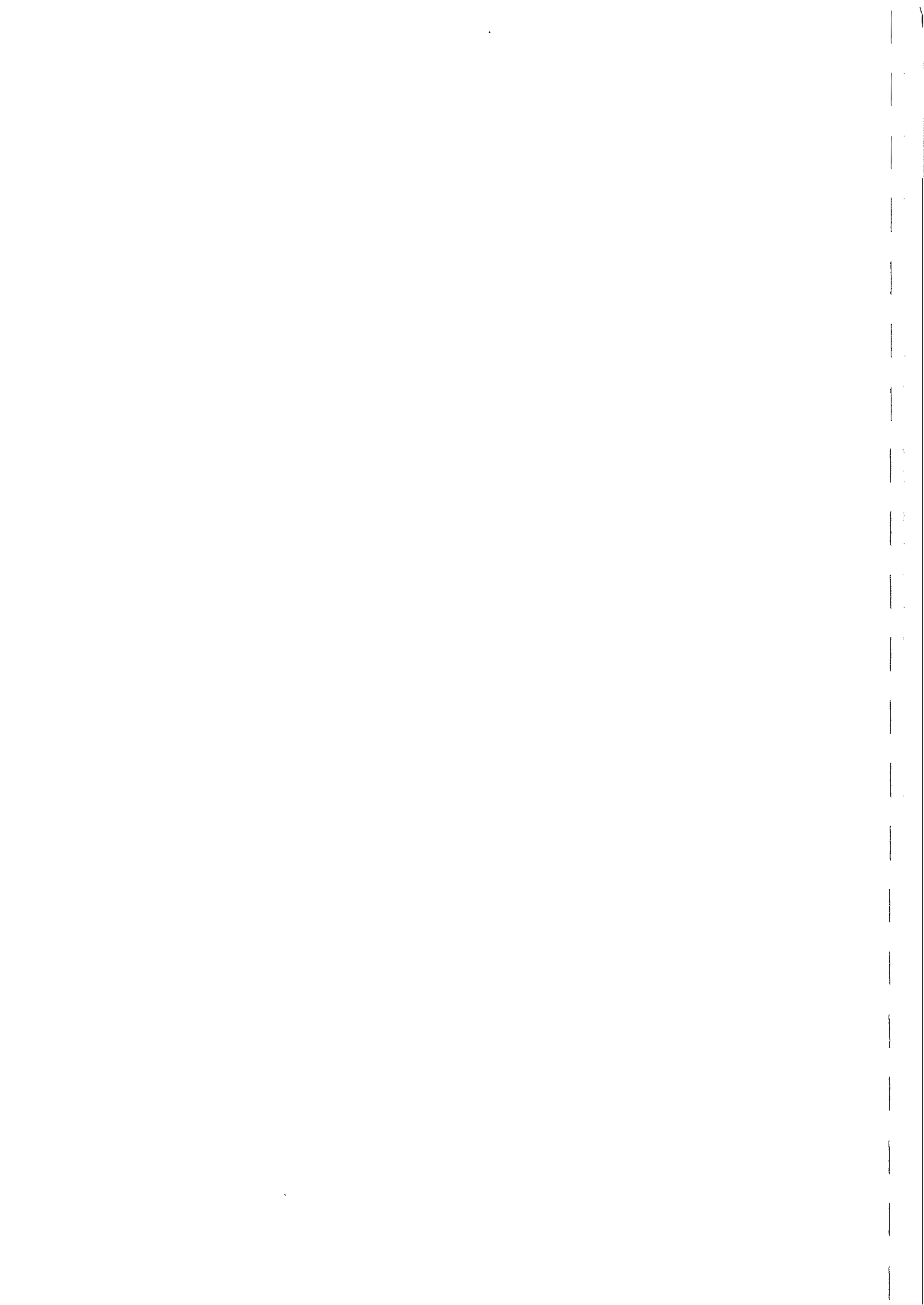
vi

Contents

1. INTRODUCTION

This report, produced within the framework of the EC funded project SCARCOST (Sumer et al, 1998), looks at scale effects in the physical modelling of seabed scour around coastal and offshore man-made structures. Scour is defined as the erosion caused by the presence of a structure and is to be distinguished from the erosion that would have occurred if the structure was not present. The report is not intended to provide an introduction to the scale modelling of waves or waves around structures with fixed beds, although the main hydrodynamic parameters are introduced below as they are also important for mobile bed studies. A thorough review of physical modelling techniques can be found in Hughes (1993) and the recent books by Hoffmans and Verheij (1997) and Whitehouse (1998) discuss the physical modelling of scour.

This report summarises the additional scale effects present in mobile bed non-cohesive sediment models when structures are added. It starts with an introduction to some of the issues involved with fixed-bed model scaling and the scaling of mobile sediments. A section on the factors that are affected by scaling is followed by a number of examples of the problems associated with specific structure types. Then a number of the features of scale model experiments are discussed.

1.1 Short wave fixed-bed model scaling

Short wave models are scaled using the following criteria, (see Hughes, 1993, for details).

- The model is geometrically undistorted, so all lengths are scaled by the geometric lengthscale, n_L $=L_p/L_m$, where L is a length and the subscripts p and m denote prototype and model.
- The Froude number, F_r, is preserved:

$$F_r = \frac{U^2}{gL},$$ (1)

  where U = velocity, g = acceleration due to gravity and L = length.
- Wave periods are scaled by Froude time scale, $n_T = \sqrt{n_L}$.
- Reynolds number scaling is important if viscous effects are to be scaled (but turbulent shear stresses do not scale by the Froude number so Reynolds number scaling is not normally achieved). The Reynolds number is

$$Re = \frac{UL}{v}$$ (2)

  where v = kinematic viscosity of the water. Hughes (1993) suggests that the viscous effects can be discounted in coastal structure models for a depth-based $Re \geq 1 \times 10^4$. However the Reynolds number is important up to values of about 2×10^5 when considering drag coefficients for flow round piles.

- Currents are also scaled by Froude number (current periods by Froude time scale).
- The turbulence level may change when a wave is superimposed on a current (the flow may even be relaminarised). This may be important in reproducing field turbulence in the laboratory (Lodahl et al. 1998).
- Rough turbulent boundary layers in model and prototype will be dynamically similar.
- Froude number similitude under waves does not lead to accurately scaled bed friction or laminar boundary layer streaming and laminar boundary layer shear stresses in the model.

Bed roughness should be scaled by geometric length scale if model is to be geometrically undistorted. This is often not possible. Moreover, as the roughness length is often taken as proportional to the median diameter of the bed material or scour protection, it implies that the sediment diameter should be scaled by the geometric length scale. This will not normally be the case, especially for small diameters. The scaling of sediment will be discussed later.

1.2 Sediment transport scaling

Some basic scaling issues for mobile sediment models, with and without structures, are outlined below. This is followed by the introduction of some of the common non-dimensional numbers used in mobile bed tests without structures. References by Hughes (1993), Oumeraci (1994) and Whitehouse (1998) are particularly useful. The choice of scaling depends on whether the flow is dominated by waves or by currents. It is assumed that processes will be wave dominated in the SCARCOST project.

The dominant mode of sediment transport in the prototype can be bedload or suspended load or possibly both. The model should have the same dominant mode of sediment transport as the prototype. It is not possible to scale bedload and suspended load simultaneously so the modelling of situations where both occur, but neither is dominant, can at best give qualitative results. Kraus and McDougal (1996) state that combined bedload and suspended load transport is likely to occur in situations involving cross-shore and longshore transport.

The total shear stress acting on the bed is made up from skin friction, form drag and a sediment transport contribution. The skin friction acts on the grains and causes the movement. The form drag is caused by the pressure field due to the flow over bed features (such as ripples). Momentum transfer to the moving sediment grains gives rise to the sediment transport contribution. It is therefore important to be aware of how the components of shear stress vary as the bed profile and amount of sediment in suspension varies. There will be more form drag, for example, where the bed is rippled compared to when the bed is flat. Fredsøe and Deigaard (1992) and Soulsby (1997) give calculation methods for the components of shear stress.

The ratio of the horizontal pressure gradient force to the shear force on a grain in an oscillatory flow should be considered, as pressure gradients and shear forces do not scale in the same way. This can be assessed by considering the grain as a cube of side d, giving the ratio of the pressure gradient force to the shear stress force as:

$$ratio = \frac{(d\, \partial p/\partial x)d^2}{\tau d^2} \tag{3}$$

where p = pressure, x = co-ordinate in wave direction and τ = shear stress. Substituting $\partial p/\partial x = 2\pi\rho U_w^2/T$ and $\tau = \frac{1}{2}\rho f_w U_w^2$ for oscillatory flow, with ρ = density of water, U_w = wave velocity amplitude just outside boundary layer, T = wave period and f_w = friction factor. Adjusting coefficients, as the grains are not regular cubes, reduces the ratio to

$$ratio \approx \frac{d}{f_w U_w T} \tag{4}$$

The pressure gradients will also affect the flow within the bed (including effects of dilation and consolidation). This will be particularly apparent when lightweight sediments are used due to their lower density and larger diameter.

Possible failure mechanisms of the foundations (or other material around the edges of the scour hole) such as rotational slip failure should be considered. This is particularly relevant when a particular mode of potential failure has been identified in the prototype structure.

A number of non-dimensional scaling parameters can be derived for the wave dominated flow case. In order for the sediment transport to be modelled correctly all these parameters should be the same in the model as in the prototype. This is not possible if the lengthscale, $n_L \neq 1$. They include the grain size Reynolds number, Re_*, which affects the bottom boundary layer:

$$Re_* = \frac{u_* d}{v} \tag{5}$$

where u_* = shear velocity, d = grain diameter and v = kinematic viscosity. Other Reynolds numbers, such as the pile Reynolds number, Re_p, will be introduced later. The friction velocity u_* is related to the bed shear stress, τ, through the water density, ρ, by $\tau = \rho u_*^2$. The total shear stress, τ, is made up of contributions from skin friction, form drag and sediment transport. The shear velocity is commonly derived from the skin friction component of the shear stress only.

The grain-size Reynolds number can be transformed mathematically to the dimensionless grain size, D_*,

$$D_* = d \left(\frac{g(s-1)}{v^2} \right)^{1/3} \tag{6}$$

where g = gravitational acceleration, $s = \rho_s / \rho$, the specific gravity or relative density (with ρ_s = sediment density). The Shield's parameter, θ, is related to the Densimetric Froude number and relates the shear stress to the sediment. θ is defined as:

$$\theta = \frac{\tau}{g(\rho_s - \rho)d} \tag{7}$$

This parameter was plotted against the grain size Reynolds number in the original Shield's diagram for incipient motion in a current. A mathematical transformation can be made to plot threshold Shields parameter, θ_{cr}, versus dimensionless grain size, D_*, as in Soulsby (1997). The plot presented by Soulsby (1997) can be used to calculate incipient motion under waves and currents. The Shields parameter and dimensionless grain size determine whether the forcing is sufficient to move a sediment grain and must be scaled correctly or the transport rate will be incorrectly scaled. Moreover the Shields parameter can be used to determine whether the bed is rippled or not. The conditions for sediment mobility are as given in Soulsby (1997):

1. If $\theta < \theta_{cr}$ then the bed is immobile.
2. If $\theta_{cr} < \theta < 0.8$ then the bed is mobile and rippled.
3. If $\theta > 0.8$ then the bed is mobile and flat with sheet flow.

The Shields parameter can be used to determine whether the local scour around a structure will be live bed scour or clear water scour. Live bed scour occurs when the bed is mobile even away from the structure ($\theta > \theta_{cr}$ for the no-structure case of incident waves/currents only). Clear water scour occurs when the bed away from the structure is immobile and the scour only occurs near the structure ($\theta < \theta_{cr}$ for the no-structure case of incident waves/currents only). The flow speed-up and shear stress amplification around the structure causes sediment to be mobile in this area (see Whitehouse, 1998, for a review).

It is important to know whether the mobile sediment is moving in suspension or bedload. In order for grains to remain in suspension their settling velocity (or sediment fall speed), w_s, must be smaller than the upward turbulent component of velocity which is related to the skin friction shear velocity u_*. Therefore sediment will be in suspension if the relative fall speed, u_*/w_s is greater than one. An alternative fall speed parameter is the Dean number, D_w,

$$D_w = \frac{H}{w_s T} \tag{8}$$

where H = wave height and T = wave period. Irie and Nadaoka (1984) produced experimental results for sediment transport in front of a vertical reflecting wall and formulated the criterion that sand would be in suspension provided

$$\frac{U_w}{w_s} \geq 10 \tag{9}$$

where U_w = amplitude of water particle velocity at the bottom. As the fall velocity increases with sediment size it follows that fine sand is more likely to be in suspension than course sand. Lower values of U_w/w_s would produce bedload transport, provided that the local value of θ exceeds θ_{cr}. They also found that the boundary between bedload and suspended load had a slight dependency on Ursell number. Xie (1981) produced a different criterion for suspension under standing waves:

$$\frac{U_w - u_{cr}}{w_s} \geq 16.5 \text{ for suspension,} \tag{10}$$

where u_{cr} = critical velocity for incipient motion.

Hughes (1993) provides details of the pros and cons of using Shields scaling (the densimetric Froude) model, the sand model, the 'best' model and the lightweight model.

2. FACTORS AFFECTED BY SCALING

2.1 Hydrodynamics

Froude scaling will adequately change the wave height and period provided that the scale is large enough that viscosity can be ignored. The non-linearity of waves is important so the scaling of the non-linearity is important. The degree of wave non-linearity is often described by the Ursell parameter, Ur:

$$Ur = \frac{H\lambda^2}{h^3}, \tag{11}$$

where H = wave height, λ = wavelength and h = water depth. All the terms scale by the geometric scaling factor therefore Froude scaling preserves the non-linearity described by the Ursell parameter (and indeed other non-dimensional numbers such as the relative wave height and steepness).

The bed boundary layer is more likely to be turbulent in the field than in the laboratory. Moreover, the boundary layer thickness, in terms of grain diameters, is likely to be greater in the field than in the lab. Other features of the hydrodynamics scaling that affect the sediment transport scaling are the generation of vortices (by flow round structures or over ripples) and the shedding of these vortices. Note that the vortex shedding may be affected by the surface roughness. The formation of horseshoe vortices may also occur at very high Keulegan-Carpenter numbers in the laboratory.

2.2 Sediment scaling

Oumeraci (1994) states that Froude scaling should be used for all hydrodynamics but that the sediment characteristics should be scaled according to the dominant form of sediment transport. He identifies the sediment fall velocity, w_s, as the main parameter involved in determining the type of transport as it combines density, size, shape and viscosity. Oumeraci uses the Xie criterion and the Irie and Nadaoka criterion for sediment transport scaling as:

$$\left[\frac{U_w - u_{cr}}{w_s}\right]_{model} = \left[\frac{U_w - u_{cr}}{w_s}\right]_{prototype} \qquad (12)$$

and

$$\left[\frac{U_w}{w_s}\right]_{model} = \left[\frac{U_w}{w_s}\right]_{prototype} \qquad (13)$$

respectively. The Irie and Nadaoka criterion will often be sufficient as U_w is often much larger than u_{cr}. Oumeraci concludes that the sediment fall velocity scale factor, n_w, should be chosen according to the Froude velocity scale, i.e. $n_w = \sqrt{n_L}$. Hughes and Fowler (1990) stated that the cross-shore sand transport of waves on beaches could be modelled providing that the Froude scaling was used for the shallow water waves and the Dean fall speed parameter, D_w, was the same in model and prototype. Under these circumstances the sediment fall velocity scale factor should also be the Froude velocity scale. Alternatively and as is common in river modelling, the fall speed can be scaled by the skin friction shear velocity, u_* giving:

$$\left[\frac{u_*}{w_s}\right]_{model} = \left[\frac{u_*}{w_s}\right]_{prototype} \qquad (14)$$

The shear velocity is related to the upward turbulent component of velocity as in Section 1.2 and also helps to determine whether the grains are in suspension. A similar scaling using a shear velocity from the total shear stress could also be used.

The fall velocity for very small sand grains (just larger than 0.063mm) is determined by the Stokes law of viscous drag. The largest sand grains fall according to a quadratic bluff-body drag law. At intermediate sizes the fall velocity is determined by a mixture of both Stokes and quadratic drag laws. Soulsby (1997, § 8.2) reviews a number of formulae for settling velocity, giving both the equations found and their anticipated range of applicability, which is important for deciding which scaling law to use.

Sediment diameter scaling by Stokes law fall speed
The Stokes law for the fall velocity of sand is given by:

$$w_s = \frac{\nu D_*^3}{18d} = d'^2\left(\frac{g(s-1)}{18\nu}\right) \qquad (15)$$

which Hallermeier (1981) gives as applicable for non-dimensional grain size number, $D_* \le 3.4$ and van Rijn (1984) gives as valid for $D_* \le 2.5$. If sediment with the same density is used for model and prototype then in the Stokes viscous drag regime the fall velocity is proportional to the grain diameter squared. Froude scaling gives the fall velocity scale, n_w, as the square root of the geometric lengthscale, n_L. Therefore the scale factor for small diameters, n_{sd} is

$$n_{sd} = n_w^{1/2} = n_L^{1/4} \qquad (16)$$

as in Oumeraci (1994). In practice, both the density and diameter can be varied between model and prototype.

Sediment diameter scaling by quadratic bluff-body fall speed
Large values of D_* produce a quadratic bluff-body settling velocity given by:

$$w_s = \frac{avD_*^{3/2}}{d} = d^{1/2}a\sqrt{g(s-1)} \qquad (17)$$

with the constant $a = 1.05$ for Hallermeier (1981) and $a = 1.1$ for van Rijn (1984). The relative ranges of validity are $21.5 \leq D_* \leq 144$ (Hallermeier) and $D_* \geq 25.9$ (van Rijn). In the quadratic bluff-body drag regime the fall velocity is proportional to the square root of the sand grain diameter. The scale factor for large diameters, n_{ld}, is

$$n_{ld} = n_w^2 = n_L . \qquad (18)$$

Large grain sizes are scaled by the geometric scale factor.

Therefore the sediment diameter lengthscale varies with absolute sediment size. This introduces questions of compatibility, if more than one sediment size must be used, and applicability. The Stokes viscous drag is strictly valid for D_* values less than about 3.4 and the quadratic bluff-body drag for D_* values greater than 25. Consider what diameters these values correspond to for different materials in water with density, $\rho = 1027 \text{kgm}^{-3}$ and viscosity, $v = 1.36 \times 10^{-6} \text{m}^2\text{s}^{-1}$. Results are given for sand (with density, $\rho_s = 2650 \text{ kgm}^{-3}$ and $s=2.58$) coal (with density, $\rho_s = 1440 \text{ kgm}^{-3}$ and $s=1.4$) and perspex (with density, $\rho_s = 1230 \text{ kgm}^{-3}$ and $s=1.2$). The upper limit of strict applicability of the Stokes viscous lengthscale, n_{sd} (at $D_* = 3.4$) is 0.17mm for sand, 0.26mm for coal and 0.33mm for perspex. However the scaling law varies slowly away from the Stokes viscous scaling so the application of n_{sd} for most sands will introduce a small error only. The lower limit of applicability of the quadratic bluff-body drag law is at about $D_*=25$, which corresponds to a diameter of 1.2mm for sand, 1.9mm for coal and 2.4mm for perspex. .

Two examples of the scaling of sand are given in Table 1. The prototype diameters and model diameters are given by d_p and d_m (both in mm). Results are given for 2 geometric lengthscales (n_L=10 and 50) and the different prototype diameters are scaled by the lengthscale appropriate to the prototype grain diameter.

Table 1   Sediment sizes as scaled by Stokes and quadratic fall velocity

Method of scaling	d_p	d_m ($n_L = 10$)	d_m ($n_L = 50$)
n_{sd} (Stokes)	0.15	0.08	0.056
n_{ld} (quadratic)	1.5	0.15	0.03

The model diameter of the 1.5mm (prototype) grain is smaller than the model diameter of the 0.15mm (prototype) grain when the lengthscale n_L=50. This is obviously wrong and arises as the quadratic bluff-body scaling law predicts model sediment sizes that are in the Stokes viscous drag regime, where the lengthscale n_{ld} is no longer valid. The quadratic lengthscale, n_{ld}, may be used safely only when prototype and model grain diameters lie in the quadratic bluff body drag regime ($D_*>20$). It should also be borne in mind that grain sizes smaller than 0.10mm in size will be likely to experience a degree of cohesion (Whitehouse, 1998).

The application of the quadratic drag law lengthscale where it is not valid can be avoided by scaling the fall velocity by the Froude velocity lengthscale and then calculating the sediment diameter by an iterative process. This is illustrated using one of the examples above. Soulsby's (1997) formula for the fall speed of natural sands is derived from fitting 2 coefficients to the available data and is given by:

$$w_s = \frac{v}{d}\left[\left(10.36^2 + 1.049D_*^3\right)^{1/2} - 10.36\right] \qquad (19)$$

This formula covers all non-dimensional grain sizes and gives a fall velocity of 0.147m/s for the large prototype sand (d_p=1.5mm). When n_L=50 the model fall velocity becomes 0.147/$\sqrt{50}$ = 0.021m/s. The grain diameter that gives that fall velocity was found iteratively from Soulsby's formula and is d=0.20mm. The model diameter of the smaller sand grain (d_p=0.15mm scaled by the same method using n_L=50) is 0.055mm, which is smaller than the model diameter of the larger grain, but is so small the sediment will be cohesive.

Scaling the fall speed by the skin friction shear velocity is more time consuming as the skin friction velocity does not scale according to the Froude velocity lengthscale. However a skin friction velocity can be determined for waves, currents or combined wave and current flows so this method is widely applicable. The prototype conditions give the required ratio of skin friction velocity to fall speed, the flows are scaled according to the Froude criteria and a model shear stress and skin friction velocity are calculated. The sediment fall speed is determined using the prototype ratio and the diameter is calculated iteratively.

Shields parameter scaling
The dimensionless Shields parameter can be used to predict whether a grain will be immobile, mobile on a rippled bed or mobile on a flat (sheet flow) bed. It is important that the same regime exists for prototype and model. Current scour tests will reach the maximum scour depth for a Shields parameter just over the critical value, θ_{cr}, which is the highest value of θ for which the particle remains at rest. Soulsby (1997) provides this formula for critical Shields parameter as a function of the dimensionless grain size:

$$\theta_{cr} = \frac{0.30}{1+1.2D_*} + 0.055[1 - \exp(-0.020D_*)] \tag{20}$$

This can be used to determine the value of the Shields parameter that will give the maximum scour depth, for a given model dimensionless grain size. The current speed or grain size may then be adjusted to give the desired values of θ and D_*. This method of scaling will affect the length of time that it takes to reach equilibrium. When the experimental Shields number is increased from the threshold value, the sediment mobility is increased, so the length of time taken to reach equilibrium is reduced. If the length of time taken to reach equilibrium is important then the ratio of experimental to threshold Shields parameter should be maintained.

2.3 Morphological features
Ripples
Ripples tend to be relatively larger in models than in prototype. For example, ripples generated by a hydraulic smooth current are asymmetrical and are often about 1000-grain diameters in wavelength (Soulsby 1997, §7.1). Therefore when the grain diameter is not geometrically scaled on going from full scale to model the ripple wavelength also does not scale geometrically and will normally be relatively larger compared to the characteristic structure length (provided model and prototype both generate ripples). Wave generated ripples are generally symmetrical and have a wavelength governed by the wave orbital amplitude. This scales with $\sqrt{n_L}$ (if the wave height is scaled by n_L) so, for example if n_L = 50 then the model pile diameter is 1/50 of the prototype diameter whereas the model ripple length will be 1/$\sqrt{50}$ =1/7.1 of the prototype ripple length. Moreover, in prototype conditions the ripples are more likely to have been washed out (θ>0.8). Ripples tend not to form in natural sediments with grain diameters in excess of 0.8mm.

Note that dunes, sand ribbons or sandwaves may also be generated by currents and that different bedforms are due to different processes and must be scaled appropriately. This section uses ripples as an example of a bedform – it does not seek to imply that current and wave ripples are generated by the same processes, only to show that these bedforms are relatively larger in model than prototype. Ripples may then be

expected to play a much larger part in the sediment transport processes in a model than in full scale. This can manifest itself in a number of ways:

- Shielding of structures by ripples. The model ripple height will constitute a larger proportion of the diameter of a horizontal pipeline that has been geometrically scaled than in the prototype situation.
- Ripple migration. The sediment transport due to ripple migration will not necessarily scale appropriately. The volumetric bedload transport rate can be calculated from the equation

$$q_b = a\Delta V_{mig}$$

where a = constant depending on the bed porosity, Δ = ripple height and V_{mig} = migration speed.

- Ripple form drag (Soulsby 1997 §7.3). The pattern of dynamic pressure over the ripples causes form drag, which is not associated with entrainment or bedload but which is associated with turbulence bursting and the diffusion of suspended sediment. The ripples often give a roughness length of a few millimetres and contribute to the total shear stress and so can cause the dominant form of resistance felt by a tidal current.
- Ripples produce effects due to their sloping sides. Sediment particles may be entrained from a sloping bed, rather that a flat one and may be deposited onto a sloping bed rather than a flat one.
- Asymmetrical vortex shedding from ripples causes net sediment transport as shown for non-linear progressive waves by Sato and Horikawa (1986) and for non-linear standing waves by Irie and Nadaoka (1984) and Seaman and O'Donoghue (1996). Therefore there will be more transport in a model with non-linear flows where ripples are relatively large than in a prototype situation with equally non-linear flows.

The presence of ripples on the bed away from the structure does not mean that the scour results will necessarily be distorted by their presence. In some cases the velocity and shear stress amplification due to the structure will be strong enough to wash out the ripples close to the structure and that may be sufficient to stop the ripples from having an effect on the scaling. See Sumer et al. (1992b) for an example.

Beach Berm
The berm shape above MWL will be different, especially if lightweight sediments are used, rather than sand. Thus lightweight (coal) sediment is often used to model shingle beaches but not sand beaches.

2.4 Bed response

Lightweight sediment may cause scaling problems with waves as the vertical flow will be relatively large compared to the settling velocity of the sediment. There will be pressure gradient effects (as outlined in the equations earlier). The flow through the bed, especially the time-dependent permeable flow, will be greater in a lightweight model that an equivalent sand model. The lightweight model affects the groundwater flows, and the depth to the concrete base of flume or basin becomes important in the distribution of pore pressures. Electro-chemical cohesion must be negligible.

Any bed may fluidise due to quasi-static pressures, cyclic loading or poro-elasticity. In each case the bed will fluidise if the vertical pressure gradient exceeds the vertical gradient of buoyant weight of the sediment. To scale fluidisation the ratio between the two forces should be the same in model and prototype. This depends on grain diameter only in that the diameter will affect the porosity of the bed.

In all dynamic events it is necessary to consider the time scale for the dissipation of pore pressures and the resulting changes in the effective stress defined as:

$$\sigma' = \sigma - p_p \tag{21}$$

where σ' = total applied stress, p_p = pore fluid pressure and σ = effective stress between soil grains. If a load is applied suddenly an initial pore pressure is generated which then decays progressively with time. If the loading times are significantly shorter than the dissipation time then the timescale becomes important. However, sands also respond to changes in the shear stress as well as the mean stress so that reducing the

density or increasing the mean shear stress results in contraction under shear stress. Conversely, increasing the density or decreasing mean shear stress results in expansion under shear stresses. So when shear stresses are applied quickly the expansion causes an increase in the effective stresses between grains and hence in the mobilised shear strength. This acts to reduce the effects caused by loading times significantly lower than the dissipation time.

The torques involved in rotational slip failure come from the horizontal pressure gradient and the shear stress (which depends on a friction coefficient and buoyant weight per unit area). The ratio of the torques must be kept constant between model and prototype.

2.5 Structural response

The wave kinematics in front of and around the structure will be made up of incident and reflected and/or diffracted wave kinematics. To a first approximation (i.e. in linear theory for 3D irregular waves) the incident and reflected waves in front of a planar coastal structure are related through the use of a reflection coefficient spectrum and a phase shift spectrum. Sutherland and O'Donoghue (1998a) show that the phase shift on reflection may be characterised by the non-dimensional parameter $\chi = \cot\alpha \left(h_t / gT^2 \right)^{1/2}$ that will be the same for model and prototype if geometrically scaled, with $\alpha =$ wall slope and $h_t =$ depth at toe of structure. Moreover, Sutherland and O'Donoghue (1998b) show that the reflection coefficient spectrum may be characterised by a frequency-dependant Iribarren number within a spectrum. This number will be preserved in Froude scaling if the wave height is scaled by the geometric scaling factor.

These two papers show that a geometrically scaled model should exhibit the same reflection characteristics as the prototype; standard techniques exist at HR as elsewhere for scaling of structures. A model wave field that is dominated by incident and reflected waves may then be taken as representative of the prototype situation. This argument above does not take into account the effect of porosity on wave reflection coefficient or phase shift, nor does it take into account the non-linear wave-wave interactions that may be caused by reflection.

The choice of material for the model structure will affect the transmission through the structure, the porosity of the structure and its permeability. Moreover it will also affect the response of structure to the hydrodynamic forces acting on it. For example the rocking or cracking or rolling of stones or dolosse in a model will be affected by the choice of material, as will the vibration or oscillation of a pile. All these factors that affect the structural response may also affect the scouring around the structure by altering the porosity, reflection and transmission and hence the wave field around the structure or by altering the stability of the structure.

The vortex shedding at a structure will be affected by the scale of the structure relative to the flow and is mainly governed by the Keulegan-Carpenter and Reynolds numbers. Specific examples will be dealt with in the sections on the different structure types (below) but in general the type of vortex shedding and the position and strength of the vortices seen in the prototype must be reproduced in the model if the scour is to be reproduced.

The choice of materials for bed and structure will help determine the structural response to undermining. The choice of material for the structure will determine if the model structure behaves in the same way as the prototype if the prototype sediment scour is accurately reproduced in the model. Moreover, the choice of material for the bed will affect, for example, the bed porosity, which will affect the methods of scouring due to flow through the bed, such as piping. The pressure gradient effect, mentioned above, may also be incorrectly scaled if the model is designed for scour due to hydraulic processes. Another example of the bed material affecting the scour occurs for scour at a pile where the scour depth is affected if $D \leq 25 d_{50}$.

3. STRUCTURE TYPES

Problems associated with different structure types are outlined below.

3.1 Vertical pile

The two main types of vortex generated by wave/current flow around a single vertical pile are the lee-wake vortex and the horseshoe vortex. The lee-wake vortex is generated at the side edges by the separation of unstable shear layers and the horseshoe vortex is generated at the front of the pile when the recirculating downflow at the bed is wrapped around the pile, see Whitehouse (1998).

In steady currents the size and intensity of the horseshoe vortex can be related to the pile Reynolds number,

$$\mathrm{Re}_p = \frac{UD}{v} \tag{22}$$

where U = steady flow velocity, D = pile diameter and v = kinematic viscosity (Breusers et al. 1977). The pile Reynolds number is the most important number in the scaling of scour round vertical piles in a steady current, provided that the ratio of bed boundary layer thickness to pile diameter is large enough not to suppress the vortex formation.

In waves only the steady flow velocity, U, is replaced by the maximum value of the orbital velocity of the water particles at the bed (away from the pile), U_w. Single pile model test results with waves by Sumer et al. (1992b) have shown that the horseshoe vortices only appear for Keulegan-Carpenter numbers, $KC \geq 6$ with

$$KC = \frac{U_w T}{D} \tag{23}$$

where T = wave period and D = pile diameter. Moreover lee-wake vortices are only shed for $KC \geq 6$. The non-dimensional maximum scour depth S/D is parameterised by the Keulegan-Carpenter number. This occurs because the Keulegan-Carpenter number determines the size (diameter) of the lee-wake vortices formed and whether they separate from the pile or not. The strength of the lee-wake vortices affects the time-scale of the scour process. Model tests with the same Keulegan-Carpenter number as the prototype situation can be performed in the laboratory and the scour depth non-dimensionalised by the pile diameter. Tests with single piles have been performed or reviewed by Herbich et al. (1984), Sumer et al. (1992b), Sumer et al. (1993) and Kobayashi and. (1994).

The transfer of importance from horseshoe vortices to lee-wake vortices as the relative strength of the current decreases and the strength of the waves increases is not well documented.

The possible scale effects are due to inaccurate scaling of the pile diameter to depth ratio (D/h), the Shields parameter (θ), the grain size to pile diameter ratio, the ripple length to pile diameter ratio, the Reynolds number (Re) and the roughness $(k^*/D$ with k^* the surface roughness of the pile). In currents the downflow, which produces the horseshoe vortex, depends on a flow-induced pressure difference between the bed and top of the boundary layer so the strength of the vortex (and hence the scour) will depend on relative depth (Sumer et al., 1992a).

The Shields parameter calculated for the incident waves and currents determines whether the scour is live bed or clear water scour. All the Sumer, et al. (1992b) tests were with live bed conditions, for which the value of the Shields parameter (in the range 0.04 to 0.37) had no discernible effect. Moreover, the tests covered a wide range of ripple length to pile diameter ratios and the non-dimensional scour depths fell onto

the same curve, parameterised by the *KC* number, showing that the scaling of the ripples was not affecting the results. In the vicinity of the pile the velocity amplification produces a local amplification of the Shields parameter which may be sufficient to wash out the ripples in the vicinity of the pile. This would explain the fact the ripples did not affect the results. Recall that the bed is mobile and flat with sheet flow when $\theta > 0.8$ and note that shear stress amplification factors can be as high as 4 to 5 in the case of waves and of order 10 in currents (Sumer, et al 1997). Moreover, the Shields parameter is proportional to the shear stress. Shear stresses below the threshold for flat bed sheet flow may be sufficient to suppress the ripples, as the transition from rippled bed to sheet flow has not been accurately described.

The Reynolds number and the roughness of the pile will help to determine downstream flow and the position of vortex shedding (and may inhibit it altogether in some cases). This will affect the position and vorticity of the vortices and hence may be expected to alter the sediment transport. Note that the Reynolds number effects are different in currents and waves and should be looked at in terms of the different physical processes involved. Model tests that produce vortex shedding at different positions round the pile relative to the vortex shedding in the prototype tests may be expected to produce different scour patterns. Sumer, et al (1992b) however noted no Reynolds number dependency in their wave scour results (Re 3.4×10^3 to 1.1×10^5) but suggested that there may be an effect at very high Reynolds numbers (around $10^5 - 3 \times 10^5$) during the transition from subcritical to supercritical flow. The Reynolds number affects the drag and inertia coefficients of a pile in a current up to about 2×10^5.

In the field, marine fouling will alter the local pile roughness in time and is not evenly distributed with depth or even around the circumference of the pile. Roughness also affects the drag and inertia coefficients used in the Morrison equation for calculating forces on the pile.

Other considerations in scaling the scour are whether random or regular waves were used in the model tests and whether the full-scale KC number lies within the range of numbers tested in the laboratory experiments. The evidence from seawall tests (Hughes and Fowler, 1991 and Xie, 1981) is that regular waves tend to produce exaggerated scour profiles compared to those produced by irregular waves with the same period and rms surface elevation. This is likely to be the case for piles as well so results for the maximum scour depth under regular waves may be greater than the scour that would be caused by irregular waves.

3.2 Group of piles

A group of piles is a much more complicated scouring situation than a single vertical pile. The scour can be local (around a single pile) or global (or dishpan) scour which is a shallow wide depression around a group of piles, see Whitehouse (1998, chapter 2). Issues of importance for scour at multiple pile groups include:

- Relative orientation to each other and to waves and currents (may be at different angles)
- Relative spacing of the piles
- Lengthscale used to characterise a group
- Current blockage due to group (which may be a problem in a 2D flume).

Sumer and Fredsøe (1998) have attempted to produce empirical guidelines for predicting the maximum scour depth for a range of 2 pile and 3 pile cases and a 4×4 pile group. The non-dimensional scour depth was found to vary with the KC number (calculated for incident waves and a single pile) and the number and relative positions of the piles. The scale issues were reported to be the same as for the single pile case. At very low gaps between piles the maximum scour depth around a group may be characterised by a group diameter rather than a pile diameter. The point at which a group diameter rather than a pile diameter should be used is not well defined but a pile gap to diameter ratio of 1:10 has been suggested (Sumer, 1998, personal communication).

3.3 Horizontal pipelines

Sumer and Fredsøe (1990) compiled data from 4 experiments on the scour around pipelines caused by currents and found that the scour depth varied weakly with the pipeline Reynolds number and the Shields parameter, for live bed tests. The non-dimensionalised scour depth generated by waves depended most strongly on the Keulegan-Carpenter number (although it also depended on the relative height of the pipe above the undisturbed bed). They conducted some tests with a rough and a smooth pipeline and found that both pipes gave the same scour depth in waves. They also noted that in typical field conditions marine fouling covers the pipe so its surface acts as a rough wall and so the Reynolds number will have no practical effect on the vortex shedding.

Sumer and Fredsøe (1990) considered the possible shielding effect of the ripples by comparing the scour depths from 2 different cylinder diameters but at exactly the same KC number. The same scour depth was observed although the ripple dimensions were quite different compared to the pipe diameter. The ripples were therefore considered not to have shielded the pipeline in this case. The technique of comparing the results from 2 sizes of pipe at the same KC number is a good way of testing for scale effects (in situations where the scour depth depends on the KC number).

Tests have been carried out with varying depths of water and the deep water conditions were found to occur for a depth of 4 times the pipeline diameter (Whitehouse, 1998). At shallower depths the depth to pipe diameter ratio may become important.

The pressure gradients in the bed from one side of the pipeline to the other may not be accurately scaled (Scarcost task 2). These are particularly important if lightweight material is to be used in the bed. At the onset of scour, seepage flow becomes piping (Scarcost task 2). Again this is more important if a lightweight material is to be used in the bed.

Sumer et al. (1988) found that pipe vibrations increased the equilibrium scour depth, especially when the vibrations reached the bed. If pipeline vibration is possible in the prototype then a flexible pipeline should be used in the model that will also vibrate in the same regime. It may be that the natural frequency of the prototype pipeline should be scaled by the Froude time scale in the model. Bryndum, et al (1997) reported that in-line vibration amplitudes decrease as the turbulence intensity increases in certain regimes. They also report that the turbulence lengthscale is much larger (relative to pipe diameter) in the field than in the laboratory experiments. These factors may affect scaling in an (as yet) unknown way, particularly if the scour depth is related to the turbulence intensity and lengthscale.

3.4 Vertical breakwater

2D scour from perfect or partial reflection

The most commonly studied aspect of scour at vertical breakwaters is the scour in front of the toe caused by the partial standing wave pattern from the interaction of incident and reflected waves. This scour is essentially 2-dimensional away from the ends of the structures and predictions of it are discussed in Powell, 1987, Carpenter and Powell, 1998 and Powell and Whitehouse, 1998. The tests of Xie (1981) and Irie and Nadaoka (1984) show that there are two types of scour caused by 2D standing waves, namely *L*-type and *N*-type. *L*-type transport occurs when relatively fine sand is carried in suspension from the nodes to the anti-lodes (or loops). *N*-type transport occurs when relatively course sand travels as bed load from between the anti-nodes and the nodes towards the nodes.

The pattern of scour is therefore dependent on the mode of sediment transport so a successful model must have the same dominant mode of transport as the prototype. This can be judged using the criteria for suspension given by Xie (1981) and Irie and Nadaoka (1984) given in Section 1.2. The problems of total and partial reflection are discussed in Oumeraci (1994) who also shows that the prototype bottom boundary layer under waves is likely to be of the order of 100 times the median grain diameter whereas the model bottom boundary layer under waves is likely to be of the order of 10 times the median grain diameter. This may affect the scaling of bed load in particular.

Scour from regular and irregular waves
Most movable bed studies of the scour in front of seawalls have been done using regular waves (Oumeraci, 1994). The few studies that have used irregular waves include Xie (1981), Hughes and Fowler (1991) and McDougal, et al (1996). The first two show that while the scouring profile is regular and repeated for the full reflection of regular waves, the scour profile for irregular waves shows varying oscillations about the mean bed level that decay in amplitude away from the structure. This can be explained looking at the variation in velocities in front of the breakwater as shown by Hughes and Fowler (1991). It does mean that irregular waves will, in general, produce less scouring away from a structure than regular waves. Predictions of the maximum prototype scour depth from regular wave model studies may well give too high a value as the prototype waves will not be regular.

Ripple size
The asymmetric vortex shedding from ripples was shown by Seaman and O'Donoghue (1996) to be the dominant mechanism for N-type sediment transport under non-linear standing waves in a small lab flume. The results did not show whether the ripples affected the average scour profile that the ripples sat on as the tests were all done at the same scale. It may be that the ripple size mainly affected the speed at which equilibrium was reached. The effect of the ripple scaling therefore is not known.

Breaking waves
The presence of breaking waves in front of the structure would lead to increased levels of turbulence which is expected to cause an increased level of sand mobility and suspension. This will not necessarily increase the scour at a structure, as the mobile sand will cause scour only if there is a net transport out of the region. Gao and Inouchi (1998) conducted scour tests in front of a vertical breakwater using standing waves, breaking clapotis and broken clapotis. The scour was most severe for the broken clapotis and guidelines are given for determining the scour and deposition. The SCARCOST work on turbulence will also help the general understanding of the problem. The question of whether the effect of wave breaking can be scaled accurately is not one that can be answered now. If geometric scaling of the initial bed and structure are assumed then the common breaking criteria would suggest that the breaking position should be modelled quite well.

Waves at oblique angles of incidence
The effect of oblique incident waves is to create a short-crested sea state (Oumeraci, 1994). This produces a wave-driven longshore current along the lines of antinodes parallel to the wall. Oblique wave experiments have been conducted by Kamphuis, et al (1993) and 3D effect are discussed by Powell (1987) and Silvester and Hsu (1997). This current will act to produce a net movement of suspended sediment, thereby producing a different result to tests in 2D. This current will be important near the ends of the structure, where the scouring process has not received much attention.

End effects
The recent papers by Sumer and Fredsøe (1997) looked at scour near the head of vertical wall breakwater. They showed that the scour depth was governed by the Keulegan-Carpenter number of the breakwater:

$$KC = \frac{U_w T}{B} \tag{24}$$

where B is the front-to-back width of the breakwater (measured at the base for a sloping breakwater). The KC number defines the behaviour and strength of the lee-wake vortices. Three main flow regimes were found:

1. Un-separated lee-wake vortex ($KC < 1$).
2. Separated flow without a horse-shoe vortex ($1 < KC < 12$).
3. Separated flow with a horse-shoe vortex ($KC > 12$).

Sumer and Fredsøe (1997) argued that the boundaries between the main flow regimes identified from the model results would probably occur at different values of KC in prototype tests. They used Sarpkaya's (1986) results to argue that the flow round a big structure can remain un-separated at KC numbers up to 2. Moreover the KC number where the horse-shoe vortex appears is related to the boundary layer thickness divided by the length of the breakwater. As this ratio will be smaller for prototype than model tests Sumer and Fredsøe argue that the horse-shoe vortex will emerge for higher values of the KC number than found in their tests. Sumer and Fredsøe (1997) also argued that KC numbers greater than 12 were unlikely to occur in nature, so the third flow regime is not important for prototype problems. This shows the necessity of identifying the main non-dimensional numbers governing the scour and ensuring that any experiments are performed within the correct range.

Tests performed with 2 breakwater widths gave non-dimensional scour depths (S/B) that varied with KC in the same way. This implies a lack of scale effects, including little or no effect from the small-scale ripples in the tests when the breakwater width is varied by a factor of almost 3. The lack of influence from ripples may be due to the enhanced flow around the end of the structure washing out the ripples.

The time for the scour at the head of the breakwater to reach equilibrium is much less (of order 200 waves) than the time needed for the 2D toe scour to reach equilibrium (of order 10^4 waves). Tests involving both types of scour should be run until the slower one has reached equilibrium or else the comparison between the scour depths will not be comparing like with like.

Sumer and Fredsøe (1997) showed that the addition of a current to the waves had the effect of greatly increasing the scour depth. This happened because a horseshoe vortex formed, there was an effective increase in KC number in one half cycle and the current transported the entrained sediment away from end of the breakwater. This implies that currents as well as waves need to be scaled together if model test results are to be useful in predicting prototype scour profiles.

Some cross-cutting themes between 2D scour and end effects are discussed by Powell and Whitehouse (1998).

3.5   Sloping wall breakwater

Many breakwaters with sloping sides exist. The scour pattern around them depends on the interaction of incident and reflected waves around them. This is governed along the front face of the breakwater by the reflection coefficient and the phase shift on reflection (Sutherland and O'Donoghue 1998a and 1998b, as discussed in Section 2.5). The scouring at sloping structures is discussed by Powell and Whitehouse (1998).

Fredsøe and Sumer (1997) show that the scour at the head of the breakwater is caused by steady streaming, governed by the Keulegan-Carpenter number based on the front-to-back width of the breakwater, measured at the original bed level. There is also an additional scouring effect at the head of the breakwater where the waves may break over the sloping round head. This is governed by the parameter $T_p(gH_s)^{0.5}/h$, which characterises the amount of water in the plunging breaker. Irregular waves were used and live bed tests were conducted using an impermeable structure.

3.6   Rubble mound breakwater

Rubble mound breakwaters are a subset of the sloping wall breakwaters that are porous and have rough surfaces. The sizes, shapes and distribution of the stones used in the construction affect the porosity, permeability, transmission, reflection and dissipation of the structure. To a first approximation the phase shift at reflection does not appear to be affected by porosity (Sutherland and O'Donoghue, 1998a) although no tests were done using structures with very low porosity. The reflection coefficient is affected (Sutherland and O'Donoghue, 1998b) so the velocity distribution in front of and around the breakwater is

affected, as is the flow through the structure. This implies that is important to model the porosity of a rubble mound breakwater.

Suppose that a structure fails due to the scour at its head. If the scour depth scales differently from the stone size will a failure mode noted in field be reproduced in the laboratory? In other words a given KC number in prototype and model will be predicted to give the same non-dimensional scour depth (*S/B*). *B* is scaled by the geometric lengthscale therefore if the same KC is used in model and prototype the scour depth will be scaled by the geometric lengthscale. If the stone size used is not geometrically scaled then the stone size to scour depth ratio will be different in model from prototype which will affect the point at which the structure will fail by slumping into the scour pit.

4.   FEATURES OF EXPERIMENT

4.1   Process type

The objective of a series of scour tests may be to model a particular situation or it can be to do a generic series of tests on a particular type of scouring. The latter are known as process type tests and normally use a simplified bathymetry and tend to be dominated by waves or currents, in order to be able to separate out the effects due to waves from those due to currents. The principal mode of sediment transport must be the same in model and prototype. If possible, the effect of turbulence should be accurately modelled. Note that in the case of a sloping wall breakwater, for example, bedload toe scour, suspended load toe scour, plunging breaker scour and vortex shedding scour are all generated by different mechanisms and occur in different regimes. This may mean that a number of different sorts of test are needed if the effect of each scouring process is to be investigated separately.

4.2   Timescale

The time-development of the scour depth, *S(t)*, typically follows the formula (Sumer, et al 1992b, Whitehouse, 1998):

$$S(t) = S_e \left[1 - \exp\left(-\frac{t}{T} \right)^p \right] \tag{25}$$

where S_e is the equilibrium scour depth, T is the characteristic time-scale (wave period, for example) and p is a fitting coefficient, often 1. The experimenter is left with a choice of how long to run the tests. The main choices are to run the experiment until it appears to have reached an equilibrium, to run the experiment for a set value of t/T, or to run the experiment for the duration of a modelled storm (defined by the number of waves). It is important to know which option has been chosen and is being reported on.

The timescales associated with different types of scouring can be quite different. The toe scour in front of a sea wall can reach equilibrium in about 3000 waves for a shingle beach, but will take of the order of 10,000 waves to reach equilibrium on a sand beach (Powell and Whitehouse, 1998). The scour caused by lee-wake vortex shedding at the head of a thin vertical breakwater will reach equilibrium in well under 1000 waves (Sumer and Fredsøe, 1997) whereas the scour caused by streaming at the head of a rubble mound breakwater will take of the order of 10,000 waves to reach equilibrium (Fredsøe and Sumer, 1997).

4.3   Scaling lengths

Most of the formulae for predicting scour depth involve the maximum scour depth non-dimensionalised by the characteristic length of the structure. This characteristic length is easy to identify for single cylindrical piles – it is the pile diameter. Other characteristic lengths have been identified for other structures, such as the front-to-back width of a vertical breakwater and the front-to-back width of the base of a sloping-wall breakwater. It is more difficult to identify a characteristic length for irregular shapes or for groups of piles

where the characteristic length for scaling the maximum scour depth may be a pile diameter or a group diameter (see Section 3.2).

4.4 Initial bed profile

The final scour profile may depend on the initial bed profile. Most laboratory experiments start with a smooth planar bed, whereas the corresponding bed profile before a prototype event is exceedingly unlikely to be smooth and planar. Kriebel, et al (1986) modelled erosion and accretion on a planar beach and a concave beach using the same waves. The time development of each beach profile was quite different as the pattern and type of wave breaking was different. Although these tests were done without a structure and are not scour tests, they do directly illustrate the effect that the initial bed profile can play in determining the equilibrium bed profile.

This may be taken as being true for many scour tests as well, as McDougal, et al (1996) showed for the case of scour in front of a vertical wall using a numerical model. The bed profiles generated by the same waves over different initial bed slopes at the toe of a vertical wall were modelled using a version of SBEACH. The steeper beaches caused the energy to be dissipated in a narrower region, which created a deeper scour depth and a bar closer to the wall. The numerical model results show that the scour prediction depends on the initial bed profile as well as the waves and sand used. Similar conclusions were reached by Kamphuis, et al (1993).

However, this conclusion may be a result of not running the experiment (or computer model) for long enough. The timescale of the experiment will certainly change but it may be that the final equilibrium bed profile should be the same for a given sand volume, structure, wave and current conditions. Even if this is the case the choice of an initial bed profile can alter the volume of sand that is within the area of the model that is mobile. This may affect the equilibrium profile and maximum scour depth in the model.

4.5 Beach response and local scour

The beach response away from the structure may scale in a different way from the local scour caused by the structure. However it may be difficult to separate out the effects. For example, if the scour in front of a vertical wall is to be measured using an initially plane beach, the beach will respond to the waves whether a wall is there or not. The response with and without a wall will be different but it is difficult to separate the effects to identify the scour caused by the presence of the structure. The most appropriate method of testing will be to generate the equilibrium beach profile without the structure and then run the scour experiment with the structure in place (for the appropriate design conditions).

5. ACKNOWLEDGEMENTS

6. REFERENCES

Breusers, H.N.C., Nicollet, G. and Shen, H.W., 1977. "Local scour around cylindrical piers." J. Hydr. Res. 15(3) 211–252.

Bryndum, M.B., Tørum, A., Vitali, L. and Verley, R., 1997. "The Multispan project: laboratory tests on in-line VIV of pipes subjected to current loads." Proc. 16th Int Conf on Offshore Mechanics and Arctic Engineering, Yokohama, Japan, ASME, Vol V, pp 7–15

Fredsøe, J. and Deigaard, R., 1992. "Mechanics of coastal sediment transport." World Scientific Publishing, Advanced Series on Ocean Engineering, Vol. 3.

Fredsøe, J. and Sumer, B.M., 1997. "Scour at the head of a rubble-mound breakwater." Coastal Engineering, 29, 231–262.

Gao, X. and Inouchi, K., 1998. "The characteristics of scouring and depositing in front of vertical breakwaters by broken clapotis." Coastal Engrg. Japan, 40(1): 99–114.

Hallermeier, R.J., 1981. "Terminal settling velocity of commonly occurring sand grains." Sedimentology, 28: 859–865.

Herbich, J.B., Schiller, R.E., Watanabe, R.K. and Dunlap, W.A., 1984. "Seafloor scour. Design guidelines for Ocean-Founded Structures." Marcel Decker Inc., NY, 320pp.

Hoffmans, G.J.M.C. and Verheij, H.J., 1997. "Scour manual." Balkema, Rotterdam.

Hughes, S.A., 1993. "Physical models and laboratory techniques in coastal engineering." World Scientific Publishing Co., Singapore.

Hughes, S.A. and Fowler, J.E., 1990. "Midscale physical model validation for scour at coastal structures." Tech Rep CERC-90-8, USAE Waterways Experiment Station, Coastal Eng Res Centre, Vicksburg, Miss.

Hughes, S.A. and Fowler, J.E., 1991. "Wave-induced scour prediction at vertical walls." ASCE Proc. Conf. Coastal Sediments '91, pp. 1886–1899.

Irie, I. And Nadaoka, K., 1984. "Laboratory Reproduction of seabed scour in front of breakwaters." Proc. 19th ICCE, ASCE, 1715–1731.

Kamphuis, J.W., Rakha, K.A. and Jui, J., 1993. "Hydraulic model experimentation on seawalls." Proc. 23rd ICCE, ASCE, 1272-1284.

Kobayashi, T. and Oda, K., 1994. "Experimental study on developing process of local scour around a vertical cylinder." Proc. 24th ICCE, ASCE, pp 1284-1297.

Kraus, N.C. and McDougal, W.G., 1996. "The effects of seawalls on the beach: part 1, an updated literature review." J. Coastal Res. 12(3), 691–701.

Kriebel, D.L., Dally, W.R. and Dean, R.G., 1986. "Undistorted Froude model for surf zone sediment transport." Proc. 20th ICCE, ASCE, pp 1296–1310.

Lodahl, C.R., Sumer, B.M. and Fredsøe, J., 1998. "Turbulent combined oscillatory flow and current in a pipe." J. Fluid Mechanics, in print.

McDougal, W.G., Kraus, N.C. and Ajiwibowo, H., 1996. "The effect of seawalls on the beach: Part II, numerical modelling of SUPERTANK seawall tests." J. Coastal Res., 12(3) 702–713.

Oumeraci, H., 1994. "Scour in front of vertical breakwaters – review of problems." Proc. Int. Workshop on Wave Barriers in Deepwaters, PHRI, Japan, 281–307

Powell, K.A., 1987. "Toe scour at seawalls subject to wave action : a literature review." HR Wallingford Report SR 119.

Powell, K.A. and Whitehouse, R.J.S., 1998. "The occurrence and prediction of scour at coastal and estuarine structures." Proc. MAFF Conf. River and Coastal Engineers, University of Keel, UK, 1-3 July 1998.

Sarpkaya, T., 1986. "Force on a circular cylinder in viscous oscillatory flow at low Keuligan-Carpenter numbers, J Fluid Mechanics, 165, 61-71.

Sato, S. and Horikawa, K., 1986. "Laboratory study on sand transport over ripples due to asymmetric oscillatory flows." Proc. 20th ICCE, ASCE, pp 1481–1489.

Seaman, R. and O'Donoghue, T., 1996. "Beach response in front of wave-reflecting structures." Proc. 25th ICCE, Orlando, ASCE pp 2284–2297.

Silvester, R. and Hsu, J.C., 1997. "Coastal Stabilisation." World Scientific.

Soulsby, R.L., 1997. "Dynamics of marine sands." Thomas Telford Limited, London, 250 pp. ISBN 0 7297 2584 X

Sumer, B.M. and Fredsøe, J., 1990. "Scour below pipeline in waves." J. Waterway, Port, Coastal and Ocean Engrg., 116(3), 307–322.

Sumer, B.M. and Fredsøe, J., 1997. "Scour at the head of a vertical-wall breakwater." Coastal Engrg 29, 201–230.

Sumer, B.M. and Fredsøe, J., 1998. "Wave scour around a group of vertical piles." J. Waterway, Port, Coastal and Ocean Engrg, 124(5): 248–256.

Sumer, B.M., Christiansen, N., and Fredsøe, J. 1992a. "Time scale of scour around a vertical pile." Proc. 2nd Int. Offshore and Polar Engng. Conf., ISOPE, San Francisco, Vol 3, 308–315.

Sumer, B.M., Christiansen, N., and Fredsøe, J. 1993. "Influence of cross-section on wave scour around piles." J. Waterway, Port, Coastal and Ocean Engrg, ASCE, 119(5) 477–495.

Sumer, B.M., Christiansen, N., and Fredsøe, J. 1997. "The horseshoe vortex and vortex shedding around a vertical wall-mounted cylinder exposed to waves." J. Fluid Mechanics 332: 41–70.

Sumer, B.M., Fredsøe, J. and Christiansen, N., 1992b. "Scour around a vertical pile in waves." J. Waterway, Port, Coastal and Ocean Engrg, ASCE, 117(1) 15–31.

Sumer, B.M., Mao, Y. and Fredsøe, J., 1988. "Interaction between vibrating pipe and erodible bed." J. Waterway, Port, Coastal & Ocean Engrg., ASCE, 114(1), 81–92.

Sumer, B.M., Whitehouse, R.J.S. and Tørum, A., 1998. "Scour around coastal structures (Scarcost)." Proceedings, Third European Marine Science and Technology Conferences, Lisbon, 23–27 May. Vol II: Strategic Marine Research, pp 963–972.

Sutherland, J. and O'Donoghue, T., 1998a. "Wave phase shift at coastal structures." J. Waterway, Port, Coastal & Ocean Engrg., ASCE, 124(2) 90-98.

Sutherland, J. and O'Donoghue, T., 1998b. "Characteristics of wave reflection spectra." J. Waterway, Port, Coastal & Ocean Engrg., ASCE,124(6).

Whitehouse, R.J.S., 1998. "Scour at marine structures." Thomas Telford Limited, London, 216pp. ISBN 0 7297 2655 2.

Van Rijn, L.C., 1984. "Sediment transport: part 1: bed load transport; part 2: suspended load transport." ASCE J. Hydraulics Division, 110, 1431–1456 & 1613–1641.

Xie, S.L., 1981. "Scouring patterns in front of vertical breakwaters and their influence on the stability of the foundations of the breakwaters." Report, Dept of Civil Eng., Delft Uni Technology, Netherlands, 61pp.

7. NOMENCLATURE

a	fitted coefficient
d	grain diameter
d_{50}	median grain diameter
D	characteristic length of structure (e.g. pile diameter)
D_*	dimensionless grain size
$D_w = H/w_s T$	Dean number
F_r	Froude number
f_w	wave friction factor
g	acceleration due to gravity
h	water depth
h_t	water depth at toe of structure
H	height of water wave
H_s	significant wave height
$k*$	surface roughness
$KC=U_w T/D$	Keulegan-Carpenter number
L	length
$n_L = L_p/L_m$	geometric lengthscale
$n_T = \sqrt{n_L}$	Froude time scale
n_w	sediment fall velocity scale factor
p	pressure
p_p	pore fluid pressure
Re	Reynolds number
Re_p	pile Reynolds number
Re_*	grain size Reynolds number
s	specific gravity or relative density of sediment grain
S	maximum depth of scour
S_e	maximum depth of scour at equilibrium
t	time
T	characteristic timescale for scour or period of water wave
Ur	Ursell number
U_w	wave orbital velocity amplitude just outside boundary layer
$u_* = (\tau/\rho)^{1/2}$	shear velocity or friction velocity
U	velocity

V_{mig}	ripple migration velocity
w_s	settling velocity of isolated sediment grains
x	co-ordinate in direction of wave motion
Δ_r	ripple height
θ	Shields parameter
θ_{cr}	critical value of Shields parameter
λ	wavelength, λ_r = ripple wave length
ν	kinematic viscosity
ρ	density of water
ρ_s	sediment (or stone) density
σ	total applied stress
σ'	effective stress between soil grains
τ	shear stress
χ	phase shift parameter

Subscripts
m	model
p	prototype
s	sediment